Journal of Power Sources 195 (2010) 1365–1369

Contents lists available at ScienceDirect

Journal of Power Sources

journal homepage: www.elsevier.com/locate/jpowsour

Short communication

Titanium carbide nanoparticles supported Pt catalysts for methanol electrooxidation in acidic media

Yiwei Ou [a], Xiaoli Cui [a,*], Xiaoyan Zhang [a], Zhiyu Jiang [b]

[a] Department of Materials Sciences, Fudan University, No. 220 Handan Road, Shanghai 200433, China
[b] Department of Chemistry, Fudan University, Shanghai 200433, China

ARTICLE INFO

Article history:
Received 23 July 2009
Received in revised form
14 September 2009
Accepted 14 September 2009
Available online 20 September 2009

Keywords:
Titanium carbide nanoparticles
Methanol oxidation
Platinum
Carbon monoxide tolerance

ABSTRACT

Titanium carbide (TiC) nanoparticles supported Pt catalyst for methanol electrooxidation is investigated for the first time. The resultant TiC/Pt catalysts are prepared by using a simple electrodeposition to load Pt nanoparticles on TiC nanocomposite. The electrodes are characterized by scanning electron microscopy and cyclic voltammetry. It is found that the TiC/Pt catalysts help alleviate the CO poisoning effect for methanol electrooxidation with a higher ratio of the forward anodic peak current (I_f) to the reverse anodic peak current (I_b). The improvement in the catalytic performance is attributed to the fact that TiC ameliorates the tolerance to CO adsorption on Pt nanoparticles. One possible mechanism to improve the CO tolerance of Pt taking TiC as supporting material in methanol electrooxidation is also proposed. The results suggest that TiC could be practical supporting materials to prepare electrocatalysts that are suitable for the methanol electrooxidation applications.

© 2009 Elsevier B.V. All rights reserved.

1. Introduction

The direct methanol fuel cell (DMFC) has come to be considered as one of the most promising options to solve future energy problems because of its characteristics such as simple construction, easy operation and high efficiency. However, the electrooxidation of methanol is a very complex reaction involving many intermediate and poisonous species. The insufficient activity of the anode catalysts is still one of the main problems for DMFCs because pure platinum is easily poisoned by anode reaction intermediates such as CO_{ads}. Two aspects are concerned in order to improve the activity and CO tolerance of Pt catalysts. One is to alloy Pt with other transition metals such as Ru, the other is to select a novel support for electrocatalysts.

Various carbon materials were extensively employed in DMFCs. Conventionally highly conductive carbon material provides a high dispersion of metal nanoparticles and facilitates electron transfer, resulting in better catalytic activity. Vulcan carbon is one of the most widely used supports for preparing fuel cell catalysts because of its good compromise between electronic conductivity and a large surface area [1–4]. Previous researches have demonstrated that using a new carbon support with a high surface area is one potential way to improve the activity of electrocatalysts through synergistic effects. These supports include expanded graphite [5], mesocarbon microbeads [6], ordered porous carbon [7–9], graphite nanofibers [10–12], carbon nanohorns [13], films of C_{60} clusters [14], carbon nanocoils [15], carbon nanocones [16], hollow graphitic nanoparticles [17], carbon nanotubes [18–21] and so on.

Recently, a kind of "active supporting materials" has been revealed that they could have a catalytic role that contributed to the observed enhancement in the methanol or formic acid electrooxidation. For example, materials such as nitrogen containing carbon nanotube [20], ruthenium oxides/Vulcan XC-72 mixed supports [22], carbon–silica composite [23], WO_3/C [24], TiO_2 nanotubes [25], WC [26] and Fe_xC–C [27] hybrid material have been investigated. The previous results suggested the strong metal–support interaction would greatly affect the electrochemical properties of the fuel cell catalysts and alleviate the CO poisoning effect on Pt in some degree.

Titanium carbide is well-known for its high melting point, high resistance to oxidation and corrosion, good thermal and electrical conductivity [28]. The nanoparticle deposits are electrically highly conducting and electrochemically active [29]. It has been demonstrated recently that bulk TiC is an attractive electrode material for electroanalytical processes and it shows fast electron transfer in particular quinone system [30]. In this work, TiC as support of Pt catalyst for methanol electrooxidation was investigated and evaluated for the first time. Experimental results demonstrated that the tolerance of CO could be improved during methanol electrooxidation when taking TiC as support for Pt nanoparticles.

* Corresponding author. Tel.: +86 21 65642397; fax: +86 21 65642682.
E-mail address: xiaolicui@fudan.edu.cn (X. Cui).

0378-7753/$ – see front matter © 2009 Elsevier B.V. All rights reserved.
doi:10.1016/j.jpowsour.2009.09.031

2. Experimental

2.1. Reagents

Titanium carbide powders (>99% purity, 40 nm in diameter) were purchased from Kaier Company (China). Vulcan XC-72 powders (30 nm in diameter) were purchased from Cabot Corporation. Nafion (perfluorinated ion exchange resin, 5 wt% solution) was purchased from Aldrich. Hydrogen hexachloroplatinate hydrate ($H_2PtCl_6{\cdot}6H_2O$, 99.95%), methanol and sulfuric acid were obtained from Shanghai Chemical Reagent Inc. and used as received. All reagents were of analytical-grade purity. Freshly distilled-deionized (DD) water was used throughout. The electrolytes were 0.5 M H_2SO_4, 1.3 mM H_2PtCl_6 + 0.5 M H_2SO_4, and 0.5 M CH_3OH + 0.5 M H_2SO_4, which were prepared from high-purity sulfuric acid, high-purity-grade methanol, $H_2PtCl_6{\cdot}6H_2O$, and DD water, respectively.

2.2. Apparatus

The electrochemical experiments were performed with a CHI 660 electrochemical workstation (CHI Instruments, Shanghai Chenhua Company) in a conventional three-electrode system at room temperature. The modified glassy carbon (GC) electrode was used as the working electrode. A platinum wire was served as the auxiliary electrode, and a saturated calomel electrode (SCE) was used as the reference electrode. All the potentials were reported vs. SCE. The electrode surface morphology was studied using scanning electron microscopy (SEM, Philips xl 230 FEG).

2.3. Electrode modification

A 0.5 wt% Nafion solution was prepared by diluting the 5 wt% Nafion solution with DD water. A definite mass of TiC was put into the 0.5 wt% Nafion solution, which was then dispersed for 40 min via ultrasonic vibration so that the nanoparticles were completely suspended in the solvent. At last, a homogeneous black suspension solution with 2 mg mL^{-1} TiC could be obtained, and a 10 μL aliquot of this solution was dropped onto the surface of the GC electrode (3 mm in diameter, CHI Company). The coating was dried at room temperature in air for 1 h. Before the modification, the GC electrode was polished with 0.3 and 0.05 μm alumina slurries, washed with DD water and acetone in order, subjected to ultrasonic agitation for 1 min in DD water, and then dried under an air stream. In order to compare the difference between TiC and Vulcan carbon XC-72, GC electrodes modified by Vulcan carbon XC-72 was also prepared by the same procedures, and the same tests were performed on GC/XC-72/Pt electrodes.

2.4. Depositing Pt on TiC or Vulcan XC-72 carbon

Platinum particles were electrodeposited on the surface of electrodes with the chronopotentiometry method from a 1.3 mM H_2PtCl_6 + 0.5 M H_2SO_4 aqueous solution in a conventional three-electrode cell. The cathodic current was 0.02 mA and the deposition time was 400 s. The amount of deposited platinum was controlled by a deposition charge as 100% current efficiency was assumed. After platinum was deposited, the electrode was rinsed with DD water, and a series of tests were performed in 0.5 M H_2SO_4 solution with and without methanol.

2.5. CO stripping test

CO absorption was done by bubbling CO gas (>99.9% purity) through the cell at a flow rate of 150 mL min^{-1}. The working electrode was controlled at 0.10 V vs. SCE along with the continuous CO bubbling for 10 min. High-purity N_2 was then purged into the solution for 30 min in order to remove the CO traces from the gas phase before the stripping test on both GC/TiC/Pt and GC/XC-72/Pt electrodes.

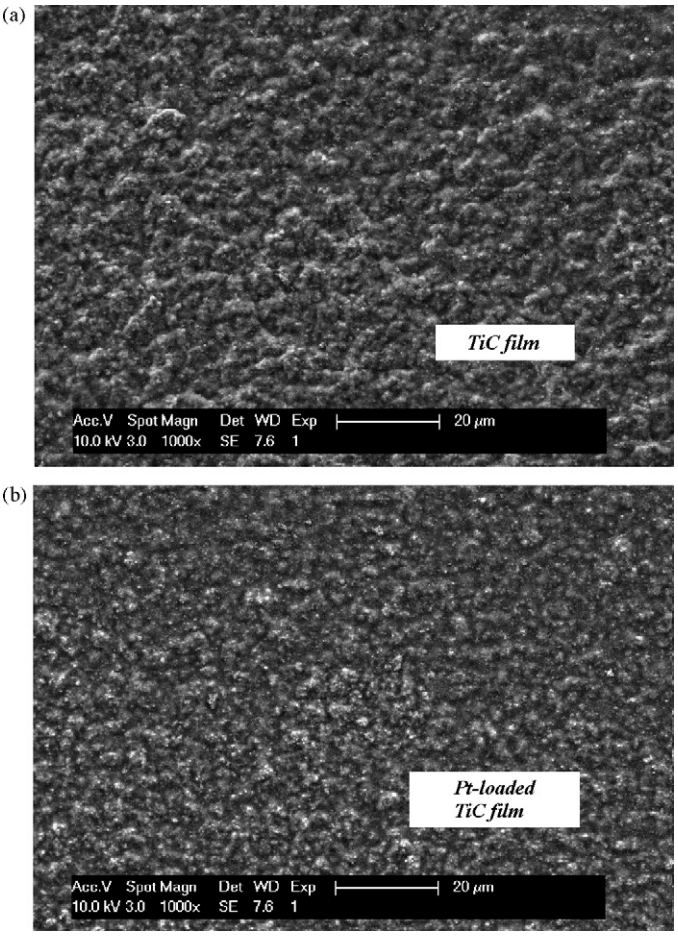

Fig. 1. The SEM images of the TiC film (a) and Pt-loaded TiC film (b) coated on glassy carbon electrode surface.

3. Results and discussion

3.1. SEM characterization of GC/TiC and GC/TiC/Pt electrodes

The typical micrographs of the TiC nanoparticles film and Pt-loaded TiC film have been investigated by scanning electron microscopy and the corresponding SEM images with the same magnification are presented in Fig. 1. From Fig. 1(a), it can be seen that the original TiC composite has a porous structure on the electrode surface. Such a structure of catalyst support will promise more platinum to be loaded and lead to good catalytic activity. The SEM image of Pt-loaded TiC film is shown in Fig. 1(b). It can be seen that tiny Pt particles scatter around the surface. The presence of platinum is also confirmed by cyclic voltammetry measurements as shown in Fig. 2.

3.2. Characterization of the electrochemical activity of the catalysts

Fig. 2 shows the cyclic voltammetry analysis on measuring the electrochemical activity in 0.5 M H_2SO_4 solution saturated by N_2 for the GC/TiC/Pt (a) and the pristine GC/TiC (b) electrode. It is interesting to observe a large oxidative peak around 0.92 V in the first cycle

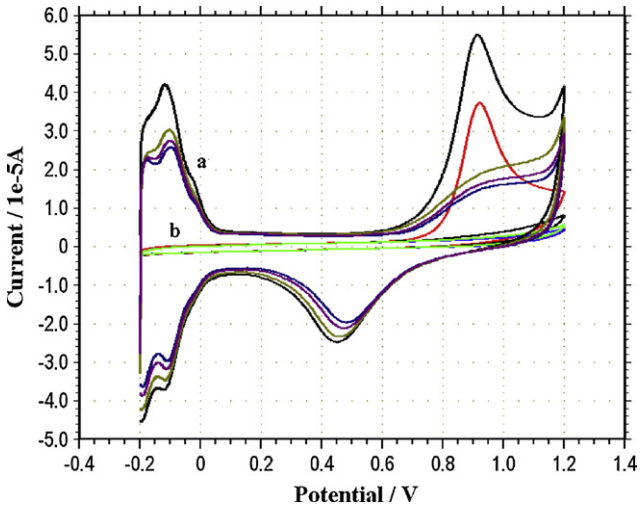

Fig. 2. Cyclic voltammetric curves of GC/TiC/Pt (a) and the pristine GC/TiC (b) electrodes at a scan rate of 0.05 V s^{-1} in 0.5 M H_2SO_4 solution saturated by N_2. The corresponding cycle number is 1, 2, 4 and 6 respectively, from outside to inside.

for GC/TiC electrodes. A clear H_2 adsorption/desorption area was identified for GC/TiC/Pt electrode (a) in the potential range from −0.20 to 0.05 V. The electrochemical active surface (EAS-H) area of Pt catalysts can be calculated from H_2 desorption area by assuming that Pt surface is covered by monolayer absorbed hydrogen and taking 0.21 mC cm^{-2} as reference [31,32]. Fig. 3 shows the cyclic voltammetry analysis on measuring the electrochemical activity in 0.5 M H_2SO_4 solution for GC/TiC/Pt (a) and GC/XC-72/Pt (b) electrodes. It was calculated that EAS-H values were about 0.15 cm^2 and 0.14 cm^2 for TiC/Pt and XC-72/Pt catalysts, respectively. The values of EAS-H indicate that GC/TiC/Pt electrode has good electrochemical activity in H_2SO_4 solution, suggesting that it may promise excellent catalytic performance [33]. These results indicate that the composites prepared by the current method can be applied as electrochemical catalysts toward methanol electrooxidation.

3.3. Electrocatalytic performance for methanol electrooxidation

The electrochemical properties of TiC/Pt catalyst have been investigated in 0.5 M CH_3OH + 0.5 M H_2SO_4 aqueous solutions. The

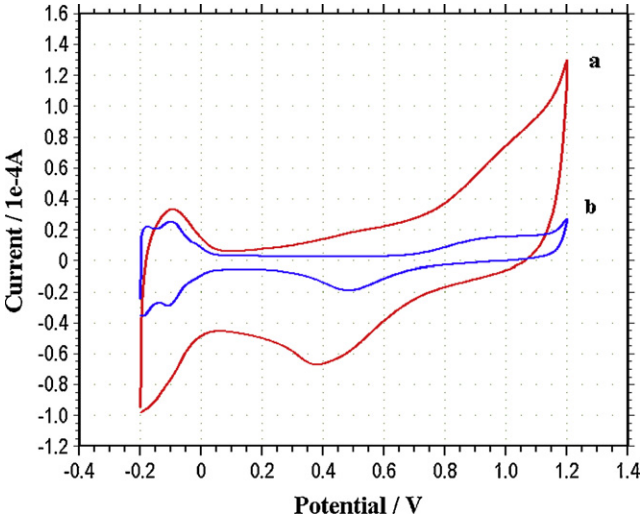

Fig. 3. Cyclic voltammetry of GC/XC-72/Pt (a) and GC/TiC/Pt (b) electrodes (second cycle) at a scan rate of 0.05 V s^{-1} in 0.5 M H_2SO_4 solution saturated by N_2.

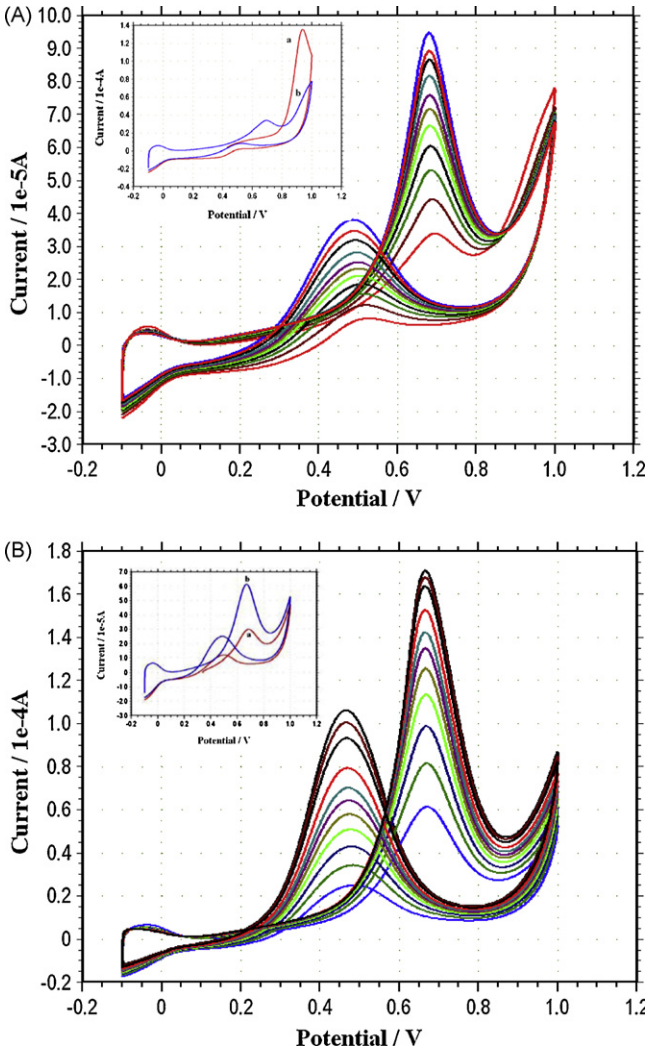

Fig. 4. A series of cyclic voltammograms of room-temperature methanol electrooxidation on GC/TiC/Pt (A) and GC/XC-72/Pt (B) electrodes with successive scanning at 0.05 V s^{-1} in 0.5 M H_2SO_4 + 0.5 M CH_3OH aqueous solutions. The corresponding cycle number is 2, 3, 4, 5, 6, 7, 8, 10, 15, 20 and 25, respectively from inside to outside. Pt loading: 57 μg cm^{-2}. The inset shows the first cycle (a) and the second cycle (b) during the cyclic scanning for the corresponding electrodes.

typical cyclic voltammograms are shown in Fig. 4(A). Before recording cyclic voltammograms, the electrode was soaked in the solution for 10 min to allow the system reaching a stable state. Fig. 4(A) shows a series of CV curves in a potential range from −0.1 to 1.0 V on successive 25 cycles. The methanol electrooxidation starts ca. 0.15 V, and the current increase is attributed to this reaction, which is represented by the anodic peak around 0.66 V. In the reverse scan, the adsorbed intermediates are further oxygenized and then produce a second oxidation peak at a potential around 0.56 V. This anodic peak in the reverse scan could be attributed to the removal of the incompletely oxidized carbonaceous species formed in the forward scan [34,35]. There are large changes during the successive potential scanning over time. The early cycles exhibit a low peak current in the forward scan and the reverse potential scan as shown in Fig. 4(A). As the number of cycles increases, the peak current increases from cycle to cycle. After scanning 10 cycles, the CV curve becomes relatively stable and the peak current increase slowly. This character of the CV curves is very typical and similar to the reports for methanol electrooxidation on Pt/C and Pt/CNTs catalysts [19,36].

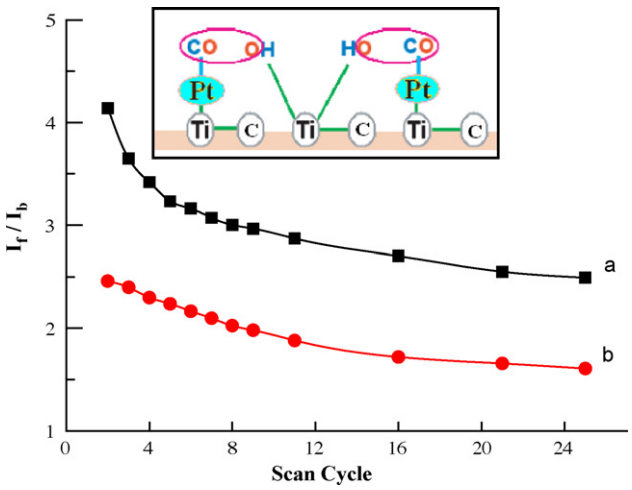

Fig. 5. The relationship between ratios of I_f/I_b vs. scanning cycle number for GC/TiC/Pt (a) and GC/XC-72/Pt (b) during methanol electrooxidation in 0.5 M H_2SO_4 + 0.5 M CH_3OH. The inset is a schematic diagram of possible mechanism for the removal of CO poisoning intermediates during methanol electrooxidation over TiC supported Pt catalysts.

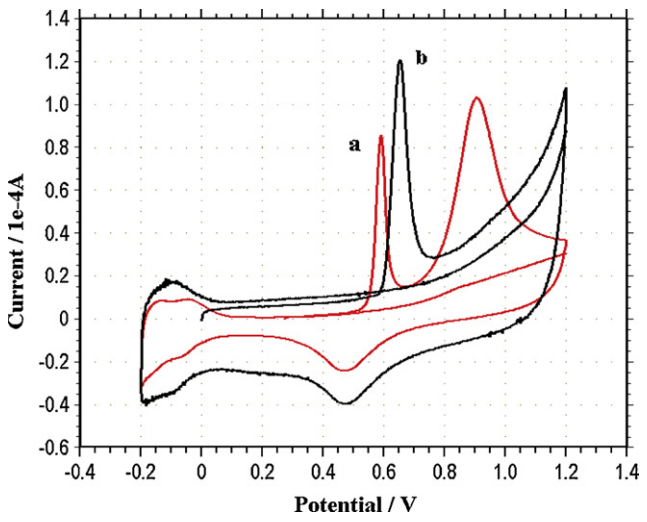

Fig. 6. The CO stripping voltammograms of GC/TiC/Pt (a) and GC/XC-72/Pt (b) electrodes scanning at 0.05 V s^{-1} in 0.5 M H_2SO_4.

A successive scanning on GC/XC-72/Pt electrodes was also performed and similar cyclic voltammetric behavior was also observed as shown in Fig. 4(B). The inset in Fig. 4(B) shows the first cycle (a) and the second cycle (b) during the cyclic scanning for the electrodes. It is worth noting the difference in the first cyclic cycle between GC/XC-72/Pt electrode and GC/TiC/Pt electrode. A large oxidative peak around 0.92 V in the first scan for GC/TiC/Pt electrode was observed as shown in the inset of Fig. 4(A). However, this oxidative peak is not present for GC/XC-72/Pt electrode in the first cycle as shown in the inset of Fig. 4(B). It is assumed that the large oxidative peak in the first scan for GC/TiC electrode may relate to the species adsorbed on TiC surface. More experiments and evidence are necessary to declare the mechanism for the large oxidative peak in the first scan.

Methanol electrooxidation on TiC/Pt and XC-72/Pt was also compared in the ratio of the forward anodic peak current (I_f) to the reverse anodic peak current (I_b) in order to indicate their catalytic performance. The ratio I_f/I_b can be used to describe the catalyst tolerance to accumulation of carbonaceous species in some degree [35–38]. High I_f/I_b value implies relatively complete oxidation of methanol to carbon dioxide. In our experiments, the ratios were measured for GC/TiC/Pt and GC/XC-72/Pt from cycle to cycle, respectively. As can be seen in Fig. 5, higher I_f/I_b values are observed for GC/TiC/Pt during the whole measured scanning process, which indicates that most of the intermediate carbonaceous species were oxidized to CO_2 in the forward scan for GC/TiC/Pt electrode. This phenomenon may be ascribed to the special properties of TiC. Further evidence was presented in CO stripping test for the two electrodes.

It should be noticed that the anodic peak current for GC/XC-72/Pt (0.17 mA) is higher than that for GC/TiC/Pt (0.095 mA) at the 50th cycle as shown in Fig. 4(A) and (B). Lower peak current of GC/TiC/Pt electrode may result from the lower electrochemical active surface area of TiC supporting material. Electrochemical tests were performed for to the pristine GC/TiC and GC/XC-72 electrodes in 0.5 M H_2SO_4 to obtain the double-layer capacitance curves (not presented in this paper). It was observed that capacitive current of GC/TiC is lower than that of GC/XC-72 when scan rates are kept at the same. It is known that capacitive current is proportional to electrochemical active surface area [32]. The catalytic activity of TiC/Pt composite may be further enhanced by decreasing the particle size of TiC to enlarge its surface area.

3.4. CO stripping results for the catalysts

The CO poisoning tolerance of TiC/Pt catalyst was further confirmed by CO stripping test. The typical results are exhibited in Fig. 6 for GC/TiC/Pt (a) and GC/XC-72/Pt (b). It is interesting to note that a large oxidative peak around 0.92 V was also observed in the first cycle for GC/TiC/Pt electrodes which is similar to the phenomenon shown in the inset of Fig. 4(A). The most notable difference between CO stripping results on GC/XC-72/Pt and GC/TiC/Pt electrodes is the negative shift of the CO oxidation peak in the latter. The onset of CO oxidation on GC/TiC/Pt electrode is shifted negatively by about 80 mV and the peak potential by about 62 mV, compared with GC/XC-72/Pt electrode. This is another indication that TiC/Pt catalyst can reduce the overpotential for CO oxidation. Besides, the charges under the CO oxidation peaks can be used to calculate EAS for Pt catalysts. By assuming a monolayer of CO on Pt surface and taking 0.42 mC cm^{-2} as reference [39], EAS-CO is 0.08 cm^{-2} (about 0.6 time of EAS-H) for GC/TiC/Pt, and 0.15 cm^{-2} (about 1.1 times of EAS-H) for GC/XC-72/Pt. As a result, the amount of CO absorbed in the surface of TiC/Pt is less than that absorbed in the surface of XC-72/Pt when loaded amount of Pt and conditions for CO bubbling are the same. Both facts have demonstrated better CO poisoning tolerance of TiC/Pt catalyst in methanol electrooxidation.

3.5. The possible mechanism

The alleviated CO poisoning effect of TiC/Pt catalyst in methanol electrooxidation has been demonstrated by the experimental facts. It may originate from formation of OH by water discharge on the TiC surface [40]. It is likely that TiC functions in the same way as Ru does in Pt–Ru/C catalysts. Similar mechanism of methanol electrooxidation on TiO_2 nanotubes supported platinum electrodes was reported recently [25]. The formation of hydroxide ion species on the surface of the TiC [40] nanoparticles transforms CO like poisoning species on Pt to CO_2, leaving the active sites on Pt for further electrochemical reaction as shown in the inset of Fig. 5. Enhanced electrocatalytic performance of methanol electrooxidation may be attributed to OH groups promoting CO removal near the Pt-oxide interface and strong metal support interaction [41]. It has been reported that the kinetics of the methanol oxidation reaction in NaOH on the platinised Ti mesh electrode was determined by the surface coverage of OH-species on the electrode surface [42].

4. Conclusions

Titanium carbide nanoparticles are employed for the supporting material of Pt catalyst in methanol electrooxidation. In comparing to Vulcan XC-72 carbon, a higher ratio of I_f/I_b during methanol electrooxidation process is observed for TiC. The CO stripping result also supports that TiC particles help alleviate CO poisoning effect on Pt catalysts. This improvement may be ascribed to the formation of OH from water on the TiC surface which ameliorates the tolerance to CO adsorption of Pt. More experimental and theoretical studies are needed to further improve the catalytic performance and identify clearer mechanisms leading to the enhancement of CO tolerance on TiC supporting material.

Acknowledgements

This work is supported by National 863 High-Tech Program of China (No. 2006AA05Z121), the National Science Foundation of China (Nos. 20673028 and 90406024) and the Shanghai Pujiang Program (2006). This work is partially supported by the open project program of the state key laboratory of chemical engineering, East China University of Science and Technology and by Shanghai Leading Academic Discipline Project (No. B113). Yiwei Ou thanks the financial support from Hui-Chun Chin and Tsung-Dao Lee Chinese Undergraduate Research Endowment (CURE, No. 09006). The authors also highly appreciate the referee's careful review and valuable comments, which have greatly improved the quality of the manuscript.

References

[1] Z.L. Liu, X.Y. Ling, X.D. Su, J.Y. Lee, J. Phys. Chem. B 108 (2004) 8234.
[2] Q.Y. Lu, B. Yang, L. Zhuang, J.T. Lu, J. Phys. Chem. B 109 (2005) 1715.
[3] W.H. Lizcano-Valbuena, D.C. Azevedo, E.R. Gonzalez, Electrochim. Acta 49 (2004) 1289.
[4] S.Y. Huang, S.M. Chang, C. Yeh, J. Phys. Chem. B 110 (2006) 234.
[5] A. Bhattacharya, A. Hazra, S. Chatterjee, P. Sen, S. Laha, I. Basumallick, J. Power Sources 136 (2004) 208.
[6] Y.C. Liu, X.P. Qiu, Y.Q. Huang, W.T. Zhu, Carbon 40 (2002) 2375.
[7] F.B. Su, J.H. Zeng, Y.S. Yu, L. Lv, J.Y. Lee, X.S. Zhao, Carbon 43 (2005) 2366.
[8] J. Ding, K.Y. Chan, J.W. Ren, F.S. Xiao, Electrochim. Acta 50 (2005) 3131.
[9] M.C. Gutierrez, M.J. Hortigulela, J.M. Amarilla, R. Jimenez, M.L. Ferrer, F.D. Monte, J. Phys. Chem. C 111 (2007) 5557.
[10] G.S. Chai, S.B. Yoon, J.S. Yu, Carbon 43 (2005) 3028.
[11] Z.R. Ismagilov, M.A. Kerzhentsev, N.V. Shikina, A.S. Lisitsyn, L.B. Okhlopkova, C.N. Barnakov, M. Sakashita, T. Iijima, K. Tadokoro, Catal. Today 102–103 (2005) 58.
[12] I.R. Moraes, W.J. Silva, S. Tronto, J.M. Rosolen, J. Power Sources 160 (2006) 997.
[13] J. Fan, M. Yudasaka, J. Miyawaki, K. Ajima, K. Murata, S. Iijima, J. Phys. Chem. B 110 (2006) 1587.
[14] K. Vinodgopal, M. Haria, D. Meisel, P. Kamat, Nano Lett. 4 (2004) 415.
[15] K.W. Park, Y.E. Sung, S.J. Han, Y.K. Yun, T.H. Hyeon, J. Phys. Chem. B 108 (2004) 939.
[16] B. Rajesh, K.R. Thampi, J.M. Bonard, A.J. McEvoy, N. Xanthopoulos, H.J. Mathieu, B. Viswanathan, J. Power Sources 133 (2004) 155.
[17] S. Han, Y. Yun, K.W. Park, Y.E. Sung, T. Hyeon, Adv. Mater. 15 (2003) 1922.
[18] Y. Lin, X. Cui, C.H. Yen, C.M. Wai, Langmuir 21 (2005) 11474.
[19] Y. Lin, X. Cui, C.H. Yen, C.M. Wai, J. Phys. Chem. B 109 (2005) 14410.
[20] T. Maiyalagan, B. Viswanathan, U.V. Varadaraju, Electrochem. Commun. 7 (2005) 905.
[21] C. Kim, Y.J. Kim, Y.A. Kim, T. Yanagisawa, K.C. Park, M. Endo, J. Appl. Phys. 96 (2004) 5904.
[22] K. Lasch, G. Hayn, L. Jorissen, J. Garche, O. Besenhardt, J. Power Sources 105 (2002) 305.
[23] M. Kim, S. Hwang, J.S. Yu, J. Mater. Chem. 17 (2007) 1656.
[24] Z.H. Zhang, Y.J. Huang, J.J. Ge, C.P. Liu, T.H. Lu, W. Xing, Electrochem. Commun. 10 (2008) 999.
[25] T. Maiyalagan, B. Viswanathan, U.V. Varadaraju, J. Nanosci. Nanotechnol. 6 (2006) 2067.
[26] M.K. Jeon, H. Daimon, K.R. Lee, A. Nakahara, S.I. Woo, Electrochem. Commun. 9 (2007) 2692.
[27] X. Wang, Y. Xia, Electrochem. Commun. 11 (2009) 28.
[28] Z. Ju, N. Fan, X. Ma, J. Li, X. Ma, L. Xu, Y. Qian, J. Phys. Chem. C 111 (2007) 16202.
[29] S.J. Stott, R.J. Mortimer, S.E. Dann, M. Oyama, F. Marken, Phys. Chem. Chem. Phys. 8 (2006) 5437.
[30] A. Lupu, D. Compagnone, S. Orlanducci, M.L. Terranova, V. Magearu, G. Palleshi, Electroanalysis 16 (2004) 1704.
[31] H. Song, X. Qiu, F. Li, Electrochim. Acta 53 (2008) 3708.
[32] J. Wang, G. Yin, Y. Shao, S. Zhang, Z. Wang, Y. Gao, J. Power Sources 171 (2007) 331.
[33] C.L. Lee, Y.C. Ju, P.T. Chou, Y.C. Huang, L.C. Kuo, J.C. Oung, Electrochem. Commun. 7 (2005) 453.
[34] R. Manoharan, J.B. Goodenough, J. Mater. Chem. 2 (1992) 875.
[35] T.C. Deivaraj, J.Y. Lee, J. Power Sources 142 (2005) 43.
[36] Z. Liu, X.Y. Ling, X. Su, J.Y. Lee, J. Phys. Chem. B 108 (2004) 8234.
[37] O.T.M. Musthafa, S. Sampath, Chem. Commun. 67 (2008) 67.
[38] T. Maiyalagan, J. Solid State Electrochem 13 (2009) 1561.
[39] T. Vidakovic, M. Christov, K. Sundmacher, Electrochim. Acta 52 (2007) 5606.
[40] S.V. Didziulis, P. Frantz, S.S. Perry, O. El-bjeirami, S. Imaduddin, P.B. Merrill, J. Phys. Chem. B 103 (1999) 11129.
[41] S.G. Neophytides, S. Zafeiratos, G.D. Papakonstantinou, J.M. Jaksic, F.E. Paloukis, M.M. Jaksic, Int. J. Hydrogen Energy 30 (2005) 393.
[42] E.H. Yu, K. Scott, R.W. Reeve, L. Yang, R.G. Allen, Electrochim. Acta 49 (2004) 2443.